



ARL-CR-0860 • APR 2021



# A Soft Robotic Technique for Camber Morphing Airfoils

by Bryant Nelson  
*Bennett Aerospace, Inc*  
*Raleigh, NC*

under contract W911QX-16-D-0014

Approved for public release; distribution is unlimited.

## **NOTICES**

### **Disclaimers**

The research reported in this document was performed in connection with contract/instrument W911QX-16-D-0014 with the US Combat Capabilities Development Command (DEVCOM) Army Research Laboratory (ARL).

The views and conclusions contained in this document are those of Bennett Aerospace and DEVCOM Army Research Laboratory. Citation of manufacturer's or trade names does not constitute an official endorsement or approval of the use thereof.

The US government is authorized to reproduce and distribute reprints for Government purposes notwithstanding any copyright notation hereon. The findings in this report are not to be construed as an official Department of the Army position unless so designated by other authorized documents.

Citation of manufacturer's or trade names does not constitute an official endorsement or approval of the use thereof.

Destroy this report when it is no longer needed. Do not return it to the originator.



# A Soft Robotic Technique for Camber Morphing Airfoils

by Bryant Nelson  
*Bennett Aerospace, Inc*  
*Raleigh, NC*

under contract W911QX-16-D-0014



**REPORT DOCUMENTATION PAGE**

*Form Approved*  
OMB No. 0704-0188

Public reporting burden for this collection of information is estimated to average 1 hour per response, including the time for reviewing instructions, searching existing data sources, gathering and maintaining the data needed, and completing and reviewing the collection information. Send comments regarding this burden estimate or any other aspect of this collection of information, including suggestions for reducing the burden, to Department of Defense, Washington Headquarters Services, Directorate for Information Operations and Reports (0704-0188), 1215 Jefferson Davis Highway, Suite 1204, Arlington, VA 22202-4302. Respondents should be aware that notwithstanding any other provision of law, no person shall be subject to any penalty for failing to comply with a collection of information if it does not display a currently valid OMB control number.

**PLEASE DO NOT RETURN YOUR FORM TO THE ABOVE ADDRESS.**

<b>1. REPORT DATE (DD-MM-YYYY)</b> April 2021		<b>2. REPORT TYPE</b> Contractor Report		<b>3. DATES COVERED (From - To)</b> November 2018–March 2019	
<b>4. TITLE AND SUBTITLE</b> A Soft Robotic Technique for Camber Morphing Airfoils				<b>5a. CONTRACT NUMBER</b> W911QX-16-D-0014	
				<b>5b. GRANT NUMBER</b>	
				<b>5c. PROGRAM ELEMENT NUMBER</b>	
<b>6. AUTHOR(S)</b> Bryant Nelson				<b>5d. PROJECT NUMBER</b>	
				<b>5e. TASK NUMBER</b>	
				<b>5f. WORK UNIT NUMBER</b>	
<b>7. PERFORMING ORGANIZATION NAME(S) AND ADDRESS(ES)</b> Bennett Aerospace, Inc 1 Glenwood Avenue, 5th Floor Raleigh, NC 27603				<b>8. PERFORMING ORGANIZATION REPORT NUMBER</b>	
<b>9. SPONSORING/MONITORING AGENCY NAME(S) AND ADDRESS(ES)</b> DEVCOM Army Research Laboratory ATTN: FCDD-RLW-LF Aberdeen Proving Ground, MD 21005				<b>10. SPONSOR/MONITOR'S ACRONYM(S)</b>	
				<b>11. SPONSOR/MONITOR'S REPORT NUMBER(S)</b> ARL-CR-0860	
<b>12. DISTRIBUTION/AVAILABILITY STATEMENT</b> Approved for public release; distribution is unlimited.					
<b>13. SUPPLEMENTARY NOTES</b>					
<b>14. ABSTRACT</b> The field of soft robotics strives to create compliant machines from soft, elastic materials. While many of these machines are inspired by nature and intended for human applications, the techniques can also be applied to aerodynamics. One such technique, pneumatic networks, uses a series of inflatable channels to create a bending motion. In this report, two such actuators are printed to form a bidirectional, camber morphing trailing-edge flap. Airframe morphing concepts must balance competing requirements of flexibility to morph with stiffness needed to bear the aerodynamic load. This is accomplished by using air pressure as a working fluid; the relative pressure between the two chambers determines the camber of the airfoil while the total pressure in both chambers determines the overall stiffness. New piezoelectric-based pneumatic valves have transformed the typical binary pneumatic actuator into a continuous one. This enabling technology allows rapid pressure control, which in turn enables rapid deflection and stiffness modulation that could apply to airframe control, vibration dampening, or load alleviation applications. This report covers the design, manufacturing, and benchtop evaluation of a pneumatic network-based camber morphing airfoil and attempts to gain an initial understanding of the deflection, force output, stiffness modulation, and load-carrying capacity.					
<b>15. SUBJECT TERMS</b> soft robotics, actuator, camber morphing, pneumatic networks, additive manufacturing, aerospace, stiffness modulation					
<b>16. SECURITY CLASSIFICATION OF:</b>			<b>17. LIMITATION OF ABSTRACT</b> UU	<b>18. NUMBER OF PAGES</b> 21	<b>19a. NAME OF RESPONSIBLE PERSON</b> Bryant Nelson
<b>a. REPORT</b> Unclassified	<b>b. ABSTRACT</b> Unclassified	<b>c. THIS PAGE</b> Unclassified			<b>19b. TELEPHONE NUMBER (Include area code)</b> (410) 306-1211



## Contents

---

<b>List of Figures</b>	<b>iv</b>
<b>1. Introduction</b>	<b>1</b>
1.1 Methods	2
1.2 Enabling Technology	3
<b>2. Experiment</b>	<b>3</b>
<b>3. Results</b>	<b>4</b>
<b>4. Discussion</b>	<b>8</b>
<b>5. Conclusion and Future Work</b>	<b>9</b>
<b>6. References</b>	<b>11</b>
<b>List of Symbols, Abbreviations, and Acronyms</b>	<b>12</b>
<b>Distribution List</b>	<b>13</b>

## List of Figures

---

Fig. 1	Bending through differential strain <sup>4</sup> .....	1
Fig. 2	(left) Design concept with morphing trailing edge integrated into airfoil; (right) cross section of actuator showing two independent PneuNets .....	2
Fig. 3	Exploded view of actuator fabrication.....	3
Fig. 4	Experimental setup.....	4
Fig. 5	Actuator fiducials at increasing pressure .....	5
Fig. 6	Tip deflection vs. pressure; (inset) actuator images from 0 to 2.5 bar in 0.5-bar increments.....	5
Fig. 7	Pressure vs. force; (inset) experiment setup .....	7
Fig. 8	Stiffness experiment; (inset, right) experimental setup; (inset, center diagonal) actuator at 2.5 bar and 0.09 Kg (0.2 lb), 0.23 Kg (0.5 lb), and 0.45 Kg (1.0 lb), respectively.....	7
Fig. 9	Load-carrying capacity experiment; (inset bottom) experimental setup and actuator images at 0.5 bar and 0.09 Kg (0.2 lb), 0.23 Kg (0.5 lb), and 0.45 Kg (1.0 lb), respectively; (inset top) actuator images at 2.5 bar and 0.09 Kg (0.2 lb), 0.23 Kg (0.5 lb), and 0.45 Kg (1.0 lb), respectively .....	8
Fig. 10	Actuator showing both bending modes.....	9



## 1. Introduction

---

The new field of soft robotics has recently emerged and is growing in popularity, particularly with robots that can operate safely among humans.<sup>1,2</sup> However, the techniques developed can also be applied to other fields including research on morphing airframes. One such technique, pneumatic networks (PneuNet), relies on a series of interconnected channels in an elastomer that can be inflated to produce a bending motion. This is accomplished by connecting or embedding a second material with a higher shear modulus, which constrains the expansion of the inflated elastomer resulting in differential strain (Fig. 1) that produces a bending motion.<sup>3</sup>

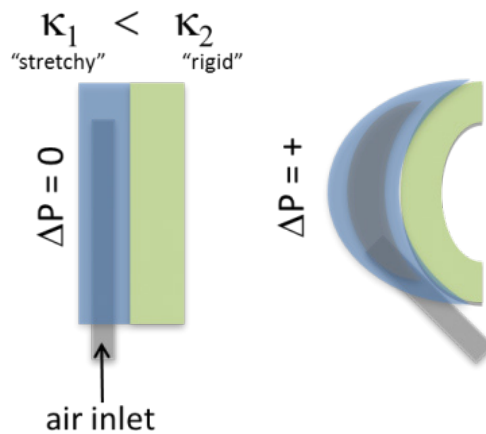
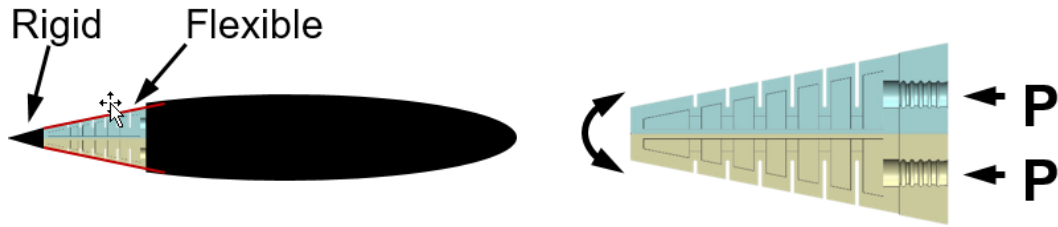


Fig. 1 Bending through differential strain<sup>4</sup>

This report will show how two PneuNets can be combined into one actuator with a form factor similar to a trailing-edge flap. The two control inputs are actuated antagonistically to bidirectionally morph (bimorph) the flap and modulate its stiffness. The relative pressure between the two chambers ( $\Delta P$ ) controls the overall bending while the total pressure ( $P_1 + P_2$ ) controls the stiffness. Certain aspects of the longer-term design have been set aside during this proof-of-concept experiment including a flexible aerodynamic skin and rigid tip (Fig. 2).



**Fig. 2** (left) Design concept with morphing trailing edge integrated into airfoil; (right) cross section of actuator showing two independent PneuNets

## 1.1 Methods

---

One of the manufacturing goals was to minimize the chance of leaks. Common PneuNet manufacturing techniques involve using an adhesive to connect two molded components; however, failures typically occur at the seam. This actuator attempted to eliminate the possibility of similar failures by 3-D printing the entire actuator. A Carbon M2 printer was selected because of the ability to print an elastomeric material (EPU 40) with a high tear strength and high elongation at break that was suitable as an actuator. This printer uses UV light to solidify the resin, followed by a thermal baking cycle that triggers a secondary chemical reaction that crosslinks the polymers and strengthens the material.<sup>5</sup>

Initial attempts at printing a monolithic actuator failed due to trapped resin inside the part during printing. The M2 printer builds parts by solidifying the material from beneath the resin vat as the build platform is slowly raised. This trapped the resin until the part was pulled entirely from the vat—identical to how an upside-down glass lifted from a tub of water traps the water in the glass until it breaks the surface. Another attempt was made by adding vent holes, which allowed the resin to drain during printing, but these holes proved difficult to seal and failed at low pressures.

A new solution was developed that took advantage of the heat-activated chemistry of EPU 40. The actuator was manufactured in two parts; then, prior to thermal curing, the two parts were placed in a jig and attached together with raw EPU 40 resin applied to the interface (Fig. 3). This ensured an air-tight seal with polymer crosslinks between both halves after the backing process.

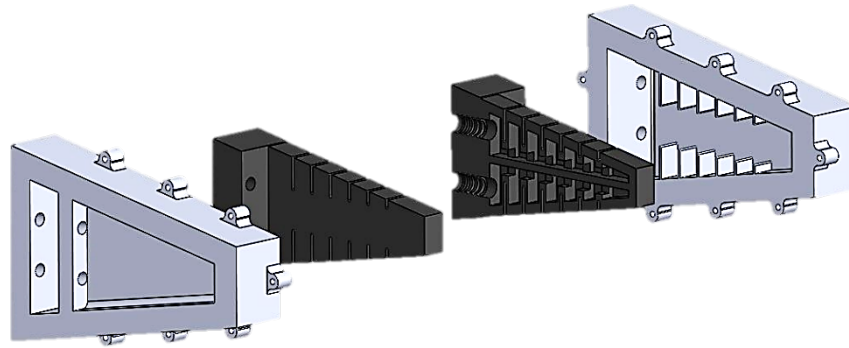


**Fig. 3 Exploded view of actuator fabrication**

PneuNets typically use a different material for a strain-limiting layer to produce a bending motion. This was achieved by thickening the midsection of the actuator to act as a “limiting” layer. However, the actuator did stretch slightly when pressurized, but this did not interfere with its operation and was only noticeable after digitally processing the image data. Future actuators produced with this technique could incorporate a channel for a second material that could be imbedded during assembly, prior to the postcure baking process.

## **1.2 Enabling Technology**

---

A key technology that enables this morphing concept is pressure modulation via high-speed piezoelectric valves. Festo, a global leader in pneumatics, has recently invented a new technology they call digital pneumatics.<sup>6</sup> Typically, pneumatic cylinders only have two stable states: fully deployed or fully retracted. The Festo Motion Terminal VTEM uses piezoelectric valves and pressure sensing for high-speed, closed-loop control that can rapidly modulate the pressure on both sides of the cylinder, which expands the binary actuation states into a continuum of states. The rapid valve actuation enables this actuator to be used for dynamic airframe control and the pressure modulation is essential for curvature control and stiffness modulation.

## **2. Experiment**

---

---

The experimental setup (Fig. 4) consisted of the actuator and camera mounted onto an optics table as well as a Festo Motion Terminal and associated computer to regulate the pressure. While this experiment could have been conducted by manually turning a regulator, the Motion Terminal offers superior pressure modulation capabilities that would be required in the future should this concept transition out of the laboratory.



**Fig. 4 Experimental setup**

Many attempts were made to produce consistent, circular fiducial markers on the black elastomer actuator. Various types of paint (spray paint, paint marker, and air brush) cracked and deteriorated over the course of operation as the material expanded and contracted. The correction fluid “Wite-Out” proved to be the most reliable and durable “paint” for the fiducial markers and persisted for all experiments without the need for reapplication.

Pneumatics tubing was fed from the Motion Terminal through undersized holes in a metal plate into the tapered gaskets printed into the actuator. The undersized holes constrained the tubing when pressurized. However, at pressures greater than 2.5 bar (36 psi), air leaked between the actuator and the inserted tubing. Therefore, all experiments were conducted up to 2.5 bar.

### **3. Results**

---

The first experiment characterized the overall displacement of the morphing flap by pressurizing Chamber 1 and leaving Chamber 2 open to ambient pressure. The tip angle was measured using the line formed by the last two fiducial points relative to those points at zero pressure to account for the tip deflection caused by the weight of the actuator. A peak deflection of  $28^\circ$  was observed at 2.5 bar. (See Figs. 5 and 6.)

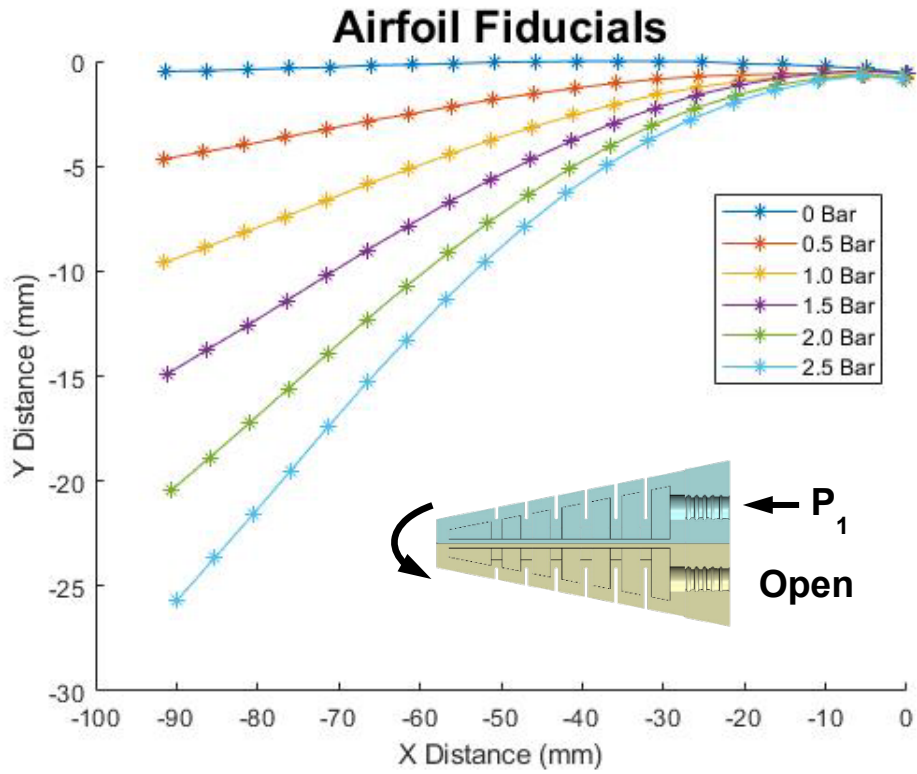


Fig. 5 Actuator fiducials at increasing pressure

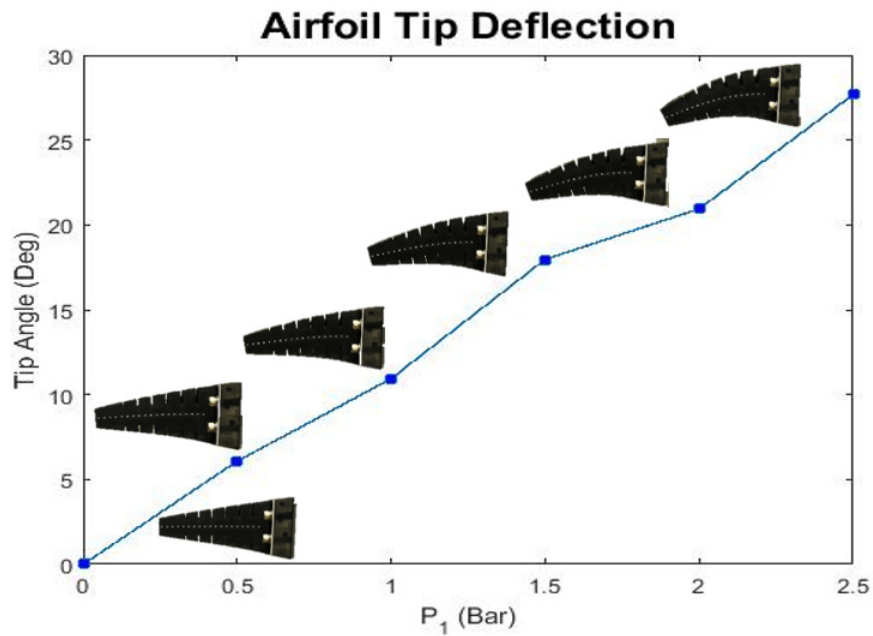


Fig. 6 Tip deflection vs. pressure; (inset) actuator images from 0 to 2.5 bar in 0.5-bar increments

To characterize the actuator force output, a load cell was placed at the tip while Chamber 1 increased in pressure. The instrument calibration was double-checked using a set of scientific test masses prior to measurements being taken. The peak force generated at 2.5 bar is 5.8 N or 1.31 pound-force.

The final set of experiments attempted to gain some understanding of the load-carrying capacity and stiffness by conducting simple experiments that could be done on the bench. While these experiments are in no way an ideal method for determining stiffness or load capacity, it was a low-cost and rapid method to gain an initial understanding of what could be expected in future experiments and quantify the stiffness modulation behavior that could be felt by hand.

The first experiment involved pressurizing both chambers identically from 0 to 2.5 bar in 0.5-bar increments and loading increasingly heavier masses (0, 0.25 oz, 0.5 oz, 0.05 lb, 0.1 lb, 0.2 lb, 0.5 lb, 1.0 lb). The load was attached to the tip of the actuator using Kapton tape and the mass of the tape was neglected during experimentation (Fig. 7). The goal of this experiment was to show the stiffness modulation capacity of the bimorph actuator that could be easily felt by hand. As expected, the highest pressure deformed the least under load and all data followed a similar trend up to the 0.23-Kg (0.5-lb) load. Under the 0.45-Kg (1-lb) load, data points for 0 and 0.5 bar diverted from the trend lines and supported the load better than the 1.0- and 1.5-bar conditions. The data was reanalyzed to confirm this unusual behavior though no definitive explanation has yet been discovered. By observing the trend lines in Fig. 8, the 0- and 0.5-bar trend lines diverge from the expected linear trajectory at the 0.45-Kg loading condition. This could have been caused by a number of factors but the most likely culprit is deformation of the interior geometry sealing and pressurizing chambers in the lower PneuNet at the lower pressure conditions. However, it is also possible that the 0- and 0.5-bar data points are indicative of the true behavior and gas leaks at higher pressures caused the actuator to underperform. It is important to note that the Festo Motion Terminal is a closed-loop system and will maintain the pressure set point in the case of small leaks.

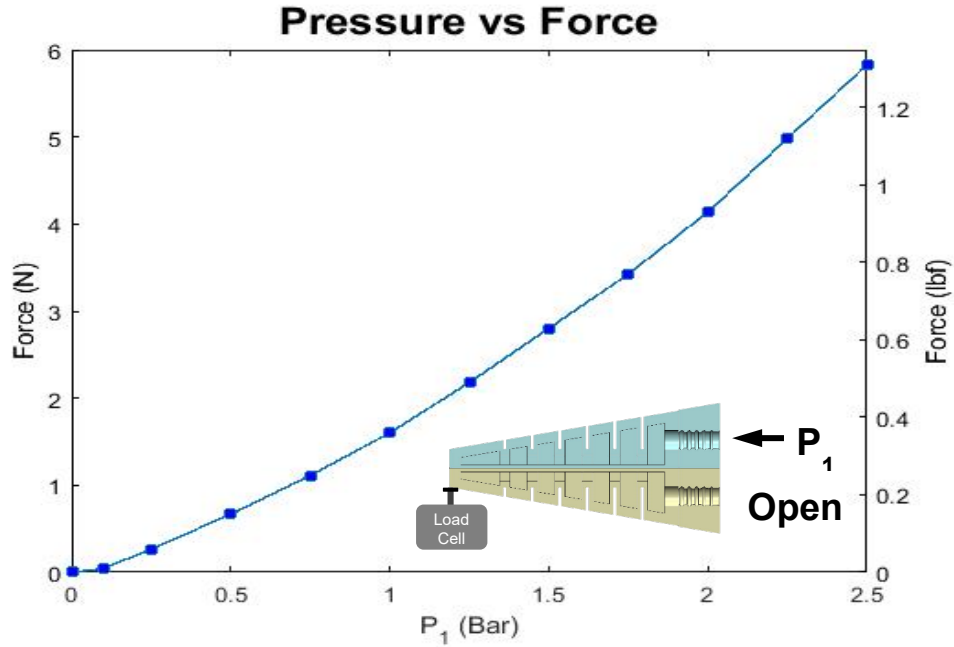


Fig. 7 Pressure vs. force; (inset) experiment setup

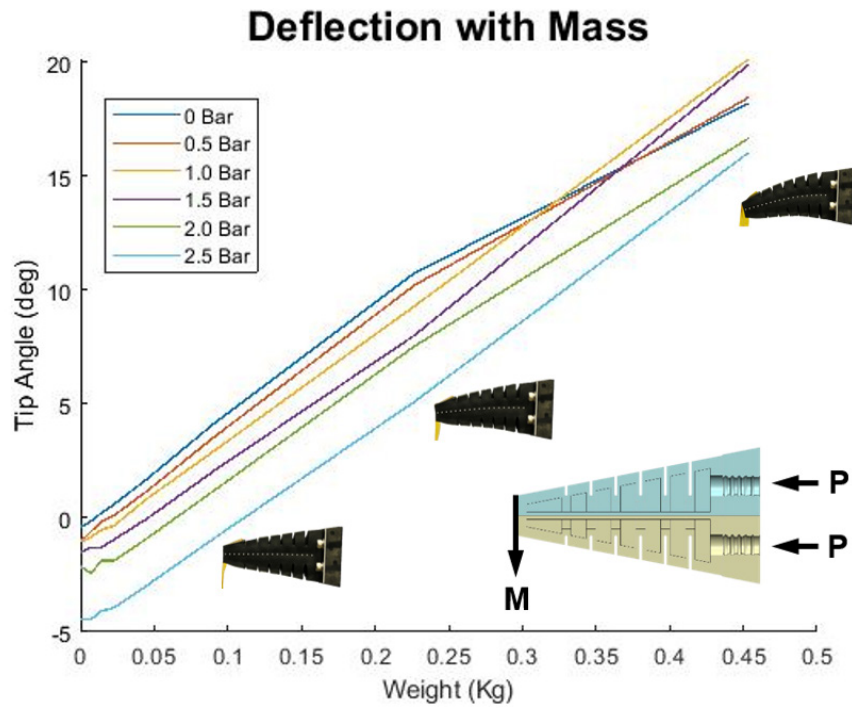


Fig. 8 Stiffness experiment; (inset, right) experimental setup; (inset, center diagonal) actuator at 2.5 bar and 0.09 Kg (0.2 lb), 0.23 Kg (0.5 lb), and 0.45 Kg (1.0 lb), respectively

The next experiment (Fig. 9) involved pressurizing Chamber 2 from 0.5 to 2.5 bar in 0.5-bar increments and loading it with the same masses. The goal of this experiment was to demonstrate the load-carrying capacity of the actuator without the need for a wind tunnel. As expected, the higher pressure better supported the applied load and no anomalies were observed.

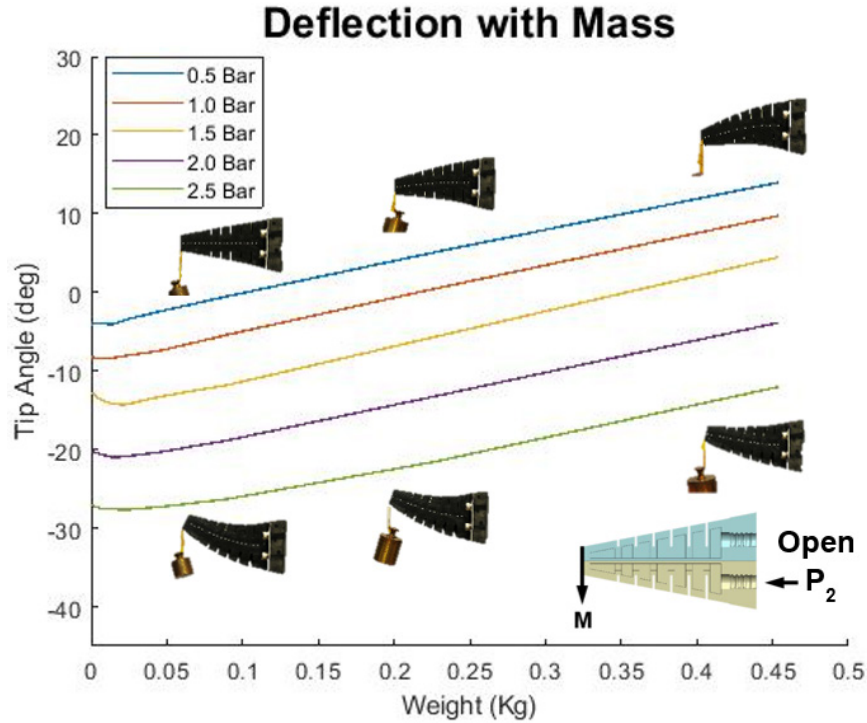


Fig. 9 Load-carrying capacity experiment; (inset bottom) experimental setup and actuator images at 0.5 bar and 0.09 Kg (0.2 lb), 0.23 Kg (0.5 lb), and 0.45 Kg (1.0 lb), respectively; (inset top) actuator images at 2.5 bar and 0.09 Kg (0.2 lb), 0.23 Kg (0.5 lb), and 0.45 Kg (1.0 lb), respectively

#### 4. Discussion

A new camber morphing technique has been demonstrated and evaluated based on soft robotic pneumatic networks. This prototype actuator exhibited significant deflection, load-carrying capacity, and stiffness modulation in benchtop experiments. The two-part actuator manufactured from EPU 40 resin showed no signs of leakage at the interface between the two printed sections. Leakage was observed around the input port at pressures greater than 2.5 bar (36 psi).

This actuator was designed by tapering a traditional pneumatic network design into a trailing edge profile. This resulted in larger chambers toward the base, which decreased in size toward the tip. This caused larger local deflections toward the base due to the larger chamber area. While this did not inhibit performance, the



internal chambers could be modified in the future to tailor the bending throughout the actuator at different pressures. As with previous pneumatic networks of similar design, there are two modes associated with bending (Fig. 10). The first mode is the expansion of the elastomer, which is constrained by the shear-limiting layer resulting in bending. The second mode is bending associated by load applied by adjacent chambers. As the cells are inflated they reach a point where they bridge the gap between the chambers, allowing load to be transferred from one chamber to the next. Since this actuator is tapered with a uniform wall thickness, the chambers toward the root contacted first due to the higher load applied to those cells. This additional mode increases the efficiency of the actuator by achieving higher deflection angles at lower pressure.

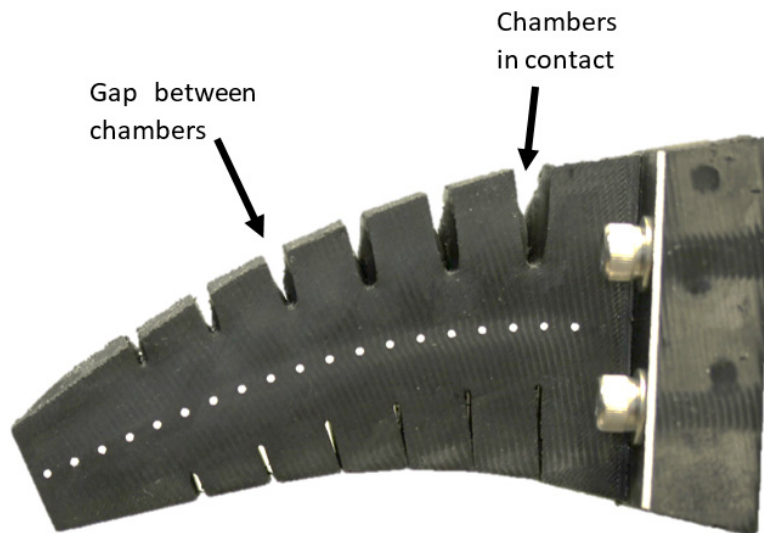


Fig. 10 Actuator showing both bending modes

## 5. Conclusion and Future Work

---

Future experimentation includes using an Instron machine to properly characterize and quantify the stiffness modulation capabilities and any observable hysteresis. Bandwidth experiments will also be conducted once the required software is obtained. It is important to note that bandwidth in pneumatic systems is highly dependent on not just the actuator but on system-level parameters such as valve speed, orifice size, and input/output tube length and geometry, among other factors. Ideally, wind tunnel experimentation will occur to obtain data under realistic loading, but such an experiment requires an aerodynamic skin to be manufactured.

New manufacturing techniques will also be investigated to expand the range of possible materials and to incorporate a rigid, instrumented core. This core will stiffen the actuator and provide feedback via strain gauges, fiber Bragg gradient,

printed piezopolymer, or other type of bending sensor. Such an actuator will be capable of closed-loop control that can be used to eliminate hysteresis-induced errors common to elastomeric actuators as well as provide additional data about the flow environment around the actuator. Such an actuator might be capable of detecting wind gusts and adapt to the flow for load alleviation or noise reduction purposes.

This new actuator concept will be evaluated to determine its suitability, limitations, and potential for a variety of applications such as commercial and military aircraft and rotorcraft (both manned and unmanned), wind turbines, race-car spoilers, rockets, and munitions.

## 6. References

---

1. Gul JZ, Sajid M, Rehman MM, Siddiqui GU, Shah I, Kim KH, Lee JW, Choi KH. 3D printing for soft robotics—a review. *Sci Tech Adv Mater.* 2018;19(1):243–262.
2. Polygerinos P, Correll N, Morin SA, Mosadegh B, Onal CD, Petersen K, Cianchetti M, Tolley MT, Shepherd RF. Soft robotics: review of fluid-driven intrinsically soft devices; manufacturing, sensing, control, and applications in human-robot interaction. *Adv Eng Mater.* 2017;19(12). <https://doi.org/10.1002/adem.201700016>.
3. Mosadegh B, Polygerinos P, Keplinger C, Wennstedt S, Shepherd RF, Gupta U, Shim J, Bertoldi K, Walsh CJ, Whitesides GM. Pneumatic networks for soft robotics that actuate rapidly. *Adv Func Mater.* 2014;24(15):2163–2170.
4. Soft Robotics Toolkit. PneuNets bending actuators. (n.d.). [accessed 2020 Dec 09]. <https://softroboticstoolkit.com/book/pneunets-bending-actuator>.
5. Carbon. DLS 3D printing technology. 2020 [accessed 2020 Dec 09]. <https://www.carbon3d.com/3d-printer-models-carbon/our-technology/>.
6. Festo. Digital pneumatics. (n.d.). [accessed 2020 Dec 09]. <https://www.festo.com/vtem/nl/cms/10169.htm>.

## List of Symbols, Abbreviations, and Acronyms

---

3-D	three-dimensional
ARL	Army Research Laboratory
bimorph	bidirectionally morph
DEVCOM	US Army Combat Capability Development Command
PneuNet	pneumatic networks
UV	ultraviolet

1 DEFENSE TECHNICAL  
(PDF) INFORMATION CTR  
DTIC OCA

1 DEVCOM ARL  
(PDF) FCDD RLD DCI  
TECH LIB

22 DEVCOM ARL  
(PDF) FCDD RLW WE  
B NELSON  
T BROWN  
B DAVIS  
D EVERSON  
M HAMAOU  
T HARKINS  
M ILG  
B KLINE  
D PETRICK  
O ROE  
B TOPPER  
FCDD RLW WD  
J BRYSON  
B BURCHETT  
I CELMINS  
J DESPIRITO  
B GRUENWALD  
C MERMAGEN  
J PAUL  
J SAHU  
L STROHM  
J VASILE  
FCDD RLW A  
F FRESCONI